Analysis and Classification of Heterogeneous Kidney Stones Using Laser-Induced Breakdown Spectroscopy (LIBS)

Belgin Genc Oztoprak,^{a,f} Jhanis Gonzalez,^b Jong Yoo,^b Turgay Gulecen,^c Nazim Mutlu,^c Richard E. Russo,^d Ozcan Gundogdu,^e Arif Demir^{e,*}

- ^a Laser Technologies Research and Application Center, Koaceli University, Kocaeli, 41275, Turkey
- ^b Applied Spectra Inc, 46661 Fremont Blvd, Fremont, CA 94558 USA
- ^c Department of Urology, Medicine Faculty, Koaceli University, Kocaeli, 41380, Turkey
- ^d Lawrence Berkeley National Laboratory, Berkeley, CA 94720 USA
- e Department of Electro-Optics System Engineering, Institute of Natural Sciences, Kocaeli University, Kocaeli, 41380, Turkey
- f BEAM Ar-Ge Optics, Laser and Spectroscopy, KOU Technopark, Kocaeli, 41275, Turkey

Kidney stones were analyzed using laser-induced breakdown spectroscopy (LIBS), utilizing a high resolution multi-channel charge-coupled device (CCD) spectrometer and a nanosecond-pulse Nd: YAG laser. The kidney stones were also characterized using X-ray diffraction (XRD) and X-ray fluorescence (XRF) techniques for comparative analysis. It was found that the ratio of hydrogen (H) to carbon (C) was an important indicator of organic compounds such as uric acid. Advantages of LIBS, especially with regards to amount of sample required and sample preparation as well as the ability to carry out elemental analysis and classification of kidney stones simultaneously, over other analytical techniques such as XRD and XRF are discussed. The common minor elements detected in the kidney stones include P, S, Si, Ti, and Zn. Principal component analysis (PCA) and partial least squares discriminant analysis (PLS-DA) of broadband LIBS spectra were employed for classifying different types of kidney stones. The results are beneficial in understanding kidney stone formation processes, which can lead to preventive therapeutic strategies and treatment methods for urological patients.

Index Headings: Laser-induced breakdown spectroscopy; LIBS; Kidney stone; X-ray diffraction; XRD; X-ray fluorescence; XRF; Principal component analysis; PCA; Partial least squares discrimination analysis; PLS-DA.

INTRODUCTION

The spectroscopic techniques using X-ray diffraction (XRD), infrared (IR) absorption, and biochemical methods have been primary analytical techniques for characterizing chemical composition of kidney stones. 1,2 However, these techniques require a relatively large quantity of sample mass for effective analysis. An alternative method that is simple, rapid, and capable of sensitive analysis based on a small quantity of sample mass is desirable. Procedures like extracorporeal shock wave lithotripsy (ESWL) or laser breaking methods are preferred in the treatment of kidney stones; as a result of these procedures, only a small amount of kidney stone material is available for analysis. The use of laserinduced breakdown spectroscopy (LIBS) has been investigated for a wide range of material analysis applications and the interest in LIBS has grown significantly due to numerous technical advantages over other analytical methods. These advantages include small sample requirements, no requirement for vacuum, minimal or no sample preparation, rapid analysis

DOI: 10.1366/12-06679

time, multi-elemental capability, and online and stand-off detection.^{3,4} Furthermore, light elements such as H, C, N, and O, which are the primary chemical constituents of organic materials, can also be analyzed using LIBS.^{5,6} Biomedical application of LIBS for analyzing teeth, bone, nail, skin, bacteria, and viruses have been reported recently.^{7–10}

The first reported study on the application of laser pulses on kidney stones was performed in 1987 when it was observed that shockwaves generated by laser ablation fragment the kidney stones into smaller pieces. The first publication on the application of LIBS for the analysis of kidney stones was reported by Fang et al.¹¹ They compared integrated spectral line intensity from 40 000 laser pulses for key elements among different kidney stones. The concentration of metallic elements in the stones was approximately estimated by assuming a linear response of measured intensities with respect to concentrations of analytes of interest in different types of kidney stones.¹¹ Singh et al. 12 investigated the elemental distribution in kidney stones versus laser focal depth at the center, at the shell, and on the surface of the kidney stones. The concentrations of Cu, Zn, Sr, and Mg in kidney stones were estimated by doping these elements at different concentrations in calcium oxalate matrix standards. The elemental concentration determined by LIBS for different kidney stones correlated well with Fourier transform infrared (FT-IR) spectroscopy¹¹ and inductively coupled plasma mass spectrometry (ICP-MS)¹² techniques. Anzano et al.¹³ identified different types of stones using two different LIBS systems, a u-LIBS and a conventional Echelle spectrometer LIBS system, both with variable laser energy. They applied linear and rank correlation methods to the LIBS spectra from the μ -LIBS system; the stones were classified using the ratios of elements based on an elemental library generated from a set of reference samples using the Echelle spectrometer LIBS system. The classification of organic and inorganic stones was compared with IR results.¹³

Like all optical emission technologies, an important aspect of LIBS is spectral data analysis and interpretation of the data; ensuring accurate identification of the measured spectral lines. For optical emission peak identification, a National Institute of Standards and Technology (NIST)¹⁴ atomic spectra database is still commonly used. However, plasma conditions under which NIST databases were generated differ from LIBS plasma excitation due to differences in temperature and electron number density. Therefore, relative intensities of atomic and ionic emission lines in the database could be inaccurate. Furthermore, dominant ionic and atomic emission lines of

Received 6 April 2012; accepted 3 August 2012.

^{*} Author to whom correspondence should be sent. E-mail: arifd@kocaeli.

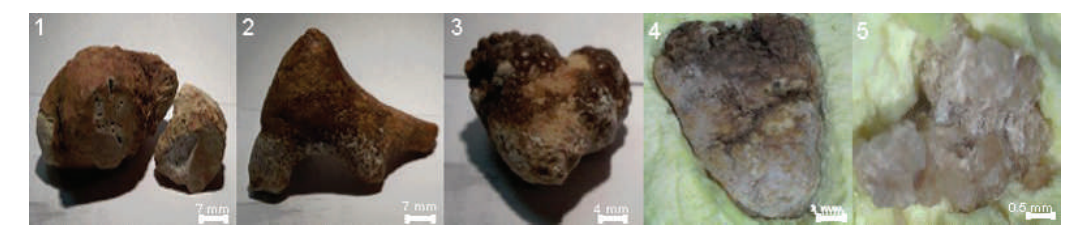


Fig. 1. Kidney stone samples taken from patients at Kocaeli University Research Hospital.

elements will be different in the LIBS plasma than in the cooler plasmas used for the NIST databases.

Advanced statistical methods are utilized for analysis of LIBS spectra and for differentiating and classifying samples. Chemometric analysis has been applied in classification of similarly structured mineral compounds of geological and biological samples. ^{15–17} Samuels et al. ¹⁶ examined bacterial spores, molds, and pollens using a broadband LIBS spectrometer with 200–980 nm spectral coverage; the spectral data were analyzed by using principal component analysis (PCA) to distinguish different biomaterials. The aim of the chemometric analysis is to identify and reduce the dimensions of complex, multi-dimensional data structures commonly measured in broadband LIBS spectra. The popular chemometric analyses for LIBS include PCA, ¹⁸ soft independent modeling of class analogy (SIMCA), ¹⁹ partial least squares discriminant analysis (PLS-DA), ²⁰ and neural network (NN) models. ²¹

The H:C ratio is considered to be a good indicator of organic structure for classification of kidney stones. The determination of organic-inorganic composition of kidney stones can be used to understand the nature of kidney stone formation and prevent stone re-formation. Kidney stones exhibit different types of crystal structure; hence, XRD analyses have been used for classification of bulk kidney stones.²² However, LIBS does not require extensive sample preparation, and analysis can be performed quickly to identify different types of kidney stones at clinics. In this study, the kidney stones collected at Kocaeli University, Faculty of Medicine during open surgeries, ESWL, and laser breaking methods were analyzed with XRD, XRF, and two LIBS instruments. The data were analyzed in each case for elemental analysis and classification of kidney stones. The elemental compositions of different kidney stones were first established by XRF. LIBS analysis of kidney stones was performed using a commercially available LIBS instrument (RT100-EC) from Applied Spectra, Inc., Fremont, CA, as well as by using a Czerny-Turner 7-channel charge-coupled device (CCD) spectrometer system (BAKI-LIBS) developed by the Laser Technologies Research and Application Center (LATARUM) at Kocaeli University, Turkey.

XRD AND XRF ANALYSIS

Figure 1 shows photographs of kidney stones obtained from Kocaeli University Faculty of Urology Department of Faculty of Medicine. As seen in the figure, some of the stones are rough and heterogeneous in appearance. XRD, FT-IR, Raman, and thermogravimetric (TGA) analyses are widely used to classify types of kidney stones. Scanning electron microscopy—energy dispersive X-ray spectroscopy (SEM-EDX) and XRF methods are used to understand their chemical compositions.²³ To determine the elemental composition and molecular crystal

structure of kidney stones, XRD and XRF analysis were performed at the Scientific and Technological Research Council of Turkey-Marmara Research Center (TUBITAK MAM).

A Shimadzu-6000 instrument was used for the XRD analysis. The kidney stones were crushed in agate mortars with maximum particle size of 325 μm based on mesh sieve. The stones were placed into an aluminum cup keeping the upper surface of the stones flat. X-ray diffraction 20 angles were measured in the range of 2° to 70° at 2°/min sensitivity. Classification of kidney stones was performed based on a pregenerated XRD kidney stone software library. A wavelength-dispersive XRF spectrometer (Philips PW-2404) was used to determine the elemental composition of kidney stones. Powder samples prepared for XRD analysis were then formed into pellets under 20 tonnes of pressure onto the special powder metal cup for XRF analysis.

LIBS ANALYSIS

Kidney stones were also analyzed by using a commercially available LIBS instrument with a 6-channel CCD spectrometer (RT100-EC LIBS instrument, Applied Spectra, Inc., Fremont, CA).²⁴ The RT100-EC integrates a Nd:YAG laser with maximum of 50 mJ energy at 1064 nm and with 5 ns pulse duration (FWHM). The system is capable of 20 Hz maximum repetition rate. Gate delay of 1 µs was selected to optimize the signal-to-noise (S/N) ratio. The samples were placed into a chamber that could be purged with different buffer gases. To maintain a consistent sample height and therefore, consistent laser spot size, the system uses auto height adjustment to account for morphological variation of the sample surface. The spot size of 150 µm was maintained at each sampled location and the laser fluence was estimated to be 113 J/cm². For each sample, fifty single-shot LIBS spectra were acquired from four different random locations, except for sample 5 due to its small size. Sample 5 was in the form of tiny solid flakes and six flakes were randomly selected and analyzed with a single laser pulse. Figure 2 shows LIBS broadband (200 to 900 nm) spectra acquired for kidney stone sample number 4. The spectral emission lines measured by LIBS are Ca, Na, Mg, K, Si, S, Ti, and Zn. The organic elements such as C, H, N and O also were detected. The intense spectral lines are identified at 247.9 nm for C; 279.7, 280.3 and 285.2 nm for Mg; 315.9, 317.9, 364.4, 370.6, 373.6, 393.4, and 396.8 nm for Ca; 766.5 and 766.9 nm for K; 330.2, 589.0, and 589.6 nm for Na; and 334.4, 334.9, and 336.1 nm for Ti.

The same kidney stones were also analyzed using the BAKI-LIBS setup²⁵ developed at Kocaeli University, LATARUM in order to demonstrate the instrumental variances that may influence measurements. Even though there are differences in the spectra, both systems can achieve classification and differentiation among stones. The Q-switched Nd:YAG laser

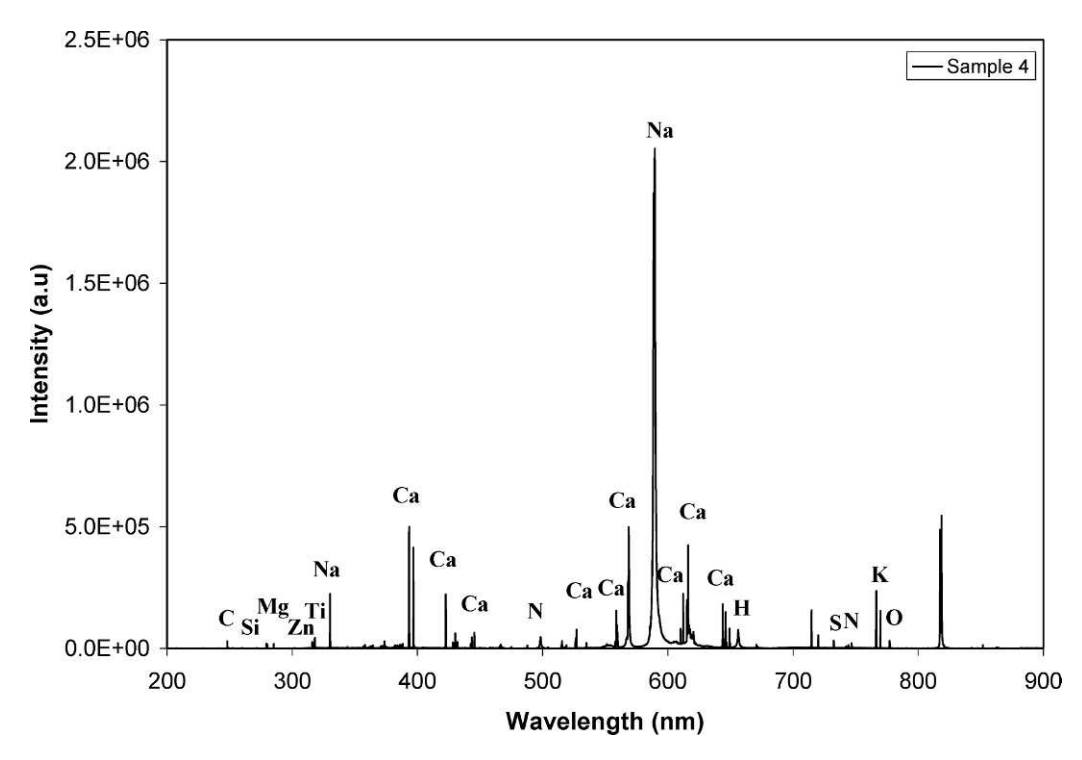


Fig. 2. LIBS spectrum of kidney stone sample 4 recorded by RT100-EC from 200 to 900 nm.

with pulse width of 4.4 ns at 1064 nm wavelength (EKSPLA NL301HT) was used for the analysis. The laser is capable of maximum energy output up to 450 mJ and can be run at the maximum repetition rate of 20 Hz. The laser beam is focused by a BK7 lens with 150 mm focal length. The laser and spectrometers were triggered and synchronized using a delay generator (DG535, Stanford Research Systems). Gate delay was 1 µs to provide an optimized S/N ratio. The emitted plasma

light was collected with a lens coupled to a 600 µm diameter fiber bundle that is split into 7 channels in a crossed Czeny—Turner type spectrometer array. The spectrometer software includes the NIST¹⁴ database for wavelength identification of LIBS emission lines. Although plasma conditions for which NIST databases were generated differ from LIBS plasma excitation due to differences in temperature and electron number density, the use of NIST database does not cause any

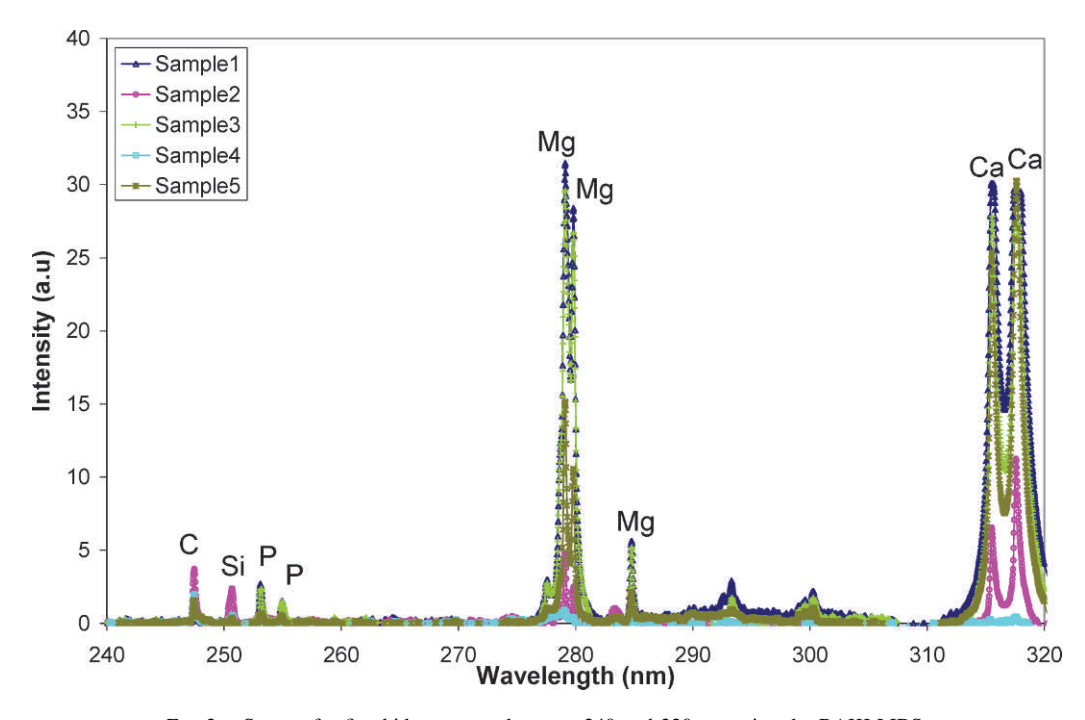


Fig. 3. Spectra for five kidney stones between 240 and 320 nm using the BAKI-LIBS.

TABLE I. XRD and XRF analysis of kidney stones.

Technique	Sample 1	Sample 2	Sample 3	Sample 4	Sample 5
XRD	Whewellite, hydroxyapatite	Whewellite, uric acid	Whewellite, wheddelite	Uric acid	Whewellite, wheddelite, hydroxyapatite
XRF	Al	Al	Al	Al	Al
	Ca	Ca	Ca	Ca	Ca
	Cl	Cl	Cl	Cl	Cl
		Fe	Fe	Fe	Fe
	K	K	K	K	K
	Mg	Mg	Mg		Mg
	-	Mo	Mo	Mo	Mo
	Na	Na	Na	Na	Na
	O	O	O	O	O
	P	P	P	P	P
	S	S	S	S	S
	Si	Si	Si	Si	Si
	Sr	Sr	Sr		Sr
					Ti
	Zn		Zn		Zn

problems in wavelength calibration, especially when experimental intensity ratios are used. Figure 3 shows LIBS spectra in the range of 240 to 320 nm for five kidney stone samples. Each spectrum was recorded with a laser energy of 150 mJ averaging over 10 shots. The spectral lines identified as 247.9 nm for C; 251.6 nm for Si; 253.6 and 255.3 nm for P; 279.7, 280.3, and 285.2 nm for Mg; and 315.9 and 317.9 for Ca. The measured spectral emission lines are from Ca, Na, Mg, K, and C as major elements and P, S, Si, Ti, and Zn as minor elements.

RESULTS AND DISCUSSION

Kidney stones were classified through the use of XRD, and their elemental composition was interrogated through the use of XRF as shown in Table I. The stones contain whewellite type compound in all samples except in sample 4. Crystal structure formation of whewellite (CaC₂O₄H₂O), wheddelite (CaC₂O₄2H₂O), hydroxyapatite Ca₁₀(PO4)₆(OH)₂, and uric acid (C₅H₄N₄O₃) compounds are found in different compositions in the stones with Ca, C, O, H, N, and P elements. However, C, H, and N could not be detected as XRF cannot identify elements with the atomic numbers Z < 8. XRF measurements determined the existence of Al, Cl, K, Na, S, and Si elements in all of the samples, whereas Fe, Mg, Mo, Sr, Ti, and Zn are only present in some of the samples. Zn was not measured in stones composed of organic uric acid. Sr in sample 2 can be observed in organic kidney stones on the order of a few parts per million (ppm).11

Besides major elements such as Ca, Mg, C, O, H, and N, low amounts of trace elements were also observed in uric acid and CaP type kidney stone samples. Trace elements are not considered to be a distinguishing mark in the classification analysis of kidney stones with the exception of P as it indicates a CaP type stone. However, the difference in trace elements is not observed in multi-compound stones, i.e., whewellite—uric acid or whewellite—hydroxyapatite type kidney stones. Anzano et al.¹³ noticed a lower intensity of inorganic elements such as Ca and Mg in the uric acid, which can be interpreted as the stones belonging to salts in urine. Ca and Mg line intensities in sample 4 are lower compared to other samples and Na line intensity is relatively higher with respect to other elements, supporting the theory that the source of the stones is salts in urine (see Fig. 2). Phosphorous observed in sample 1 was

relatively higher than the other samples, supporting the theory that these stones belong to the CaP type called hydroxyapatite.

Besides the common elements found in kidney stones such as Ca, Mg, O, Na, K, and P, elements at lower concentrations such as Ti, Zn, Al, Cl, S, Si, Fe, Mo, and Sr were measured in the XRF data. Although, the relative concentration of elements changes from sample to sample, Ca, Mg, C, H, O, Na, K, and P were also measured with both LIBS systems. Furthermore, elements present in lower concentrations such as Zn, Si, and Ti were measured with LIBS. There is a very good agreement of elemental information obtained from both LIBS emission and XRF spectra. Although Singh et al.12 measured intense Cu lines in their analysis of kidney stones, we have not detected Cu using XRF or two LIBS systems (BAKI-LIBS and RT100-EC LIBS). Meyer and Angino²⁶ observed the inhibitory effect of Cu on calcium phosphate stones but they also reported that Cu did not affect the crystal growth of calcium oxalate. Ozgurtas et al.²⁷ detected no differences relating to Cu urinary excretion between stone patients and healthy controls. However, Trinchieri et al.²⁸ found significantly higher amounts of Cu in urinary excretion of stone patients. Atakan et al.²⁹ reported that Cu might have a promoter effect on calcium oxalate stone formation. The role of Cu in the kidney stone formation process is unclear as yet, with many different explanations and suggestions in the literature. Looking at the wide variety of explanations reported, it is possible to conclude that the formation of kidney stones may be closely related to

TABLE II. Variable importance in projection (VIP) scores for each spectral wavelength in PLS calculations.

VIP scores	Wavelength	Element
22.0784	616.172	Ca
17.8505	393.393	Ca
17.4807	612.164	Ca
15.9099	616.107	Ca
14.8736	396.855	Ca
14.5548	393.316	Ca
13.7728	714.834	Ca
12.5169	558.92	Ca
12.0512	766.503	K
11.6273	317.991	Ca

TABLE III. Elemental spectral intensity line ratio analysis of kidney stone samples.

Element ratio	Whewellite, hydroxyapatite Sample 1	Whewellite, uric acid Sample 2	Whewellite, wheddelite Sample 3	Uric acid Sample 4	Whewellite, wheddelite, hydroxyapatite Sample 5
H:C	4.16±0.16	2.06±0.14	5.12±0.25	2.42±0.11	4.20±0.23
Ca:C	69.40 ± 2.31	7.83 ± 1.45	59.09 ± 9.52	0.01 ± 0.12	42.87 ± 0.65
Mg:C	18.54 ± 0.71	0.46 ± 0.01	16.80 ± 0.64	0.10 ± 0.01	7.57 ± 0.41
Ca:H	16.68 ± 0.46	3.81 ± 0.12	11.55 ± 0.41	0.01 ± 0.001	10.19 ± 0.49
Mg:H	4.46 ± 0.26	0.23 ± 0.01	3.28 ± 0.21	0.04 ± 0.01	1.80 ± 0.12
P:(P+C)	0.71 ± 0.01	nd	0.67 ± 0.01	nd	0.45 ± 0.01

and dependent on dietary habits of people and prevalent cooking methods popular in certain areas of the world.³⁰ It is known that copper pots are commonly used for cooking and copper pipes are still in use to carry water, leading to large amounts of copper accumulation in the body, especially in India and eastern regions of Turkey.³¹ A number of animal studies also confirm that the kidney is a target of copper toxicity.³² The samples examined in this study did not have any copper content.

Classification of different types of kidney stones can be made by comparing ratios of intensities of certain LIBS emission lines. In our study, the line intensity ratios of different elements were used to classify the stones as was reported by the Anzano et al.¹³ study. The spectral lines of C (247.9 nm), P (253.6 nm), Mg (279.7 nm), Ca (310.9 nm), and H (656.7 nm) were used to calculate the intensity ratios. Peak smoothing by an adjacent averaging method, line-shape fitting with the Lorentzian function, and background subtraction were applied to the spectral lines. Elemental ratios of the samples were calculated to generate the data library relevant for the kidney stones analyzed in this study. The classification of kidney stones was made based on the ratios of spectral line intensity as summarized in Table III. As the excitation and ionization energy changes from element to element, line intensities vary in LIBS measurement as a function of laser intensity. Singh et al. 12 reported that the emitted intensity of Sr from kidney stone is dependent on laser energy. When line intensity ratio is used in classification of kidney stones, laser energies have to be taken into account since temperature, electron number density, and therefore excitation condition of the plasma strongly depend on total laser energy coupled to the target surface.

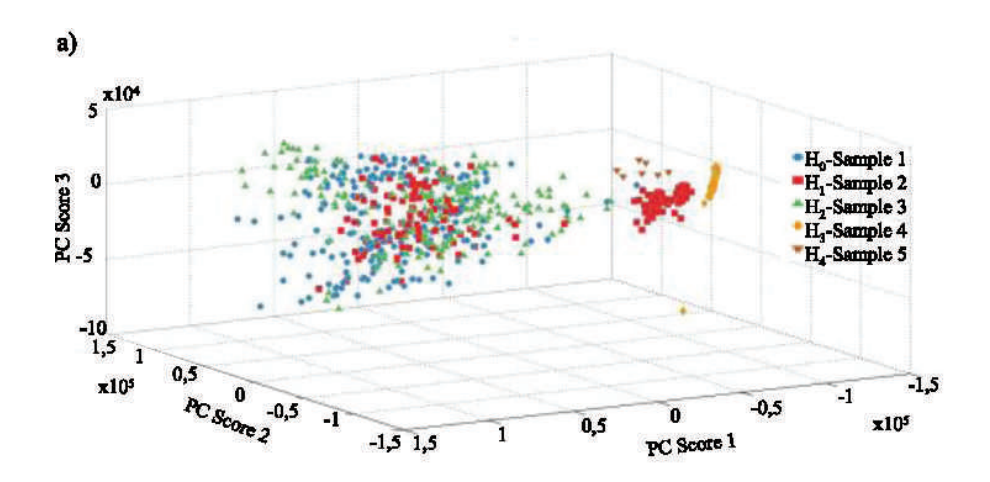
By considering spectral line intensity ratios of selected elements, it can be determined whether the kidney stones have organic or inorganic compounds. The ratio of H to C is an important criterion for differentiating inorganic from organic compounds such as uric acid. 13,33,34 In samples 2 and 4, the ratio of H to C was relatively low compared to the other samples. Higher Ca and P amounts indicate existence of CaP component, helping to distinguish calcium phosphate (hydroxyapatite) from calcium oxalate (whewellite) as seen in sample 1 in Table III. When CaP type stones are compared with CaO type stones, the ratio of Ca to C in sample 1 is higher than the other samples, although sample 3 shows similar ratios of Ca/C and P/(P+C) despite the fact that these ratios are higher than for sample 5. We have employed XRD in order to investigate the samples further for the presence of crystallite structures. However, XRD results have shown no CaP crystal structure for sample 3 despite the fact that LIBS data show the presence of CaP. The presence of P has also been confirmed further through the use of XRF. This may also be due to the fact that XRD has a lower detection sensitivity when compared to LIBS or the disadvantage of XRD not being able to measure amorphous samples. The ratio of Mg to C in samples containing CaP compounds is higher than in samples 2 and 4. A high LIBS intensity of P emission lines indicates that the stones are of CaP type.

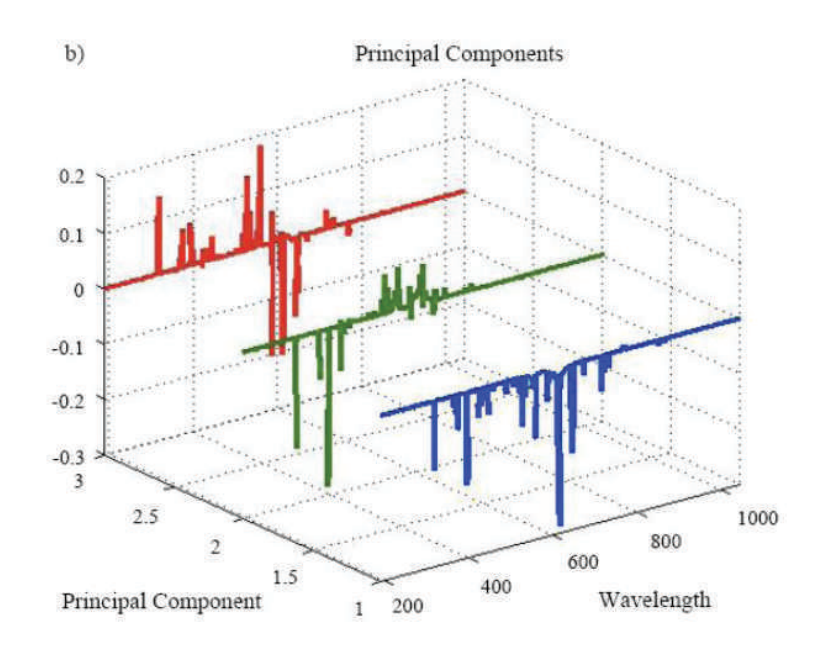
Partial least squares discriminant analysis is used for sample classification using a highest confidence approach.³⁵ Chemometric analysis of our samples was performed using PCA and PLS-DA. The PCA and PLS-DA analysis for the spectra of five different kidney stones obtained using the RT100-EC LIBS instrument is seen in Fig. 4. The PCA and PLS-DA analyses were performed based on commercially available chemometric software LIBS Graphical Development Tool (LIBS GDT) (New Folder Consulting). The PCA plot displays the spectral data along projected vectors (or "principal components") in which there is a high variance of the original data. The principal components are numbered in the order of greatest variance (PC 1) to lesser variance among the data points (PC 2, 3, 4...n). In the current study, seventeen principal components were calculated and the first three principal components were used to visualize the kidney stone sample classification in Fig. 4a.

The PCA loading plot is shown in Fig. 4b to highlight the weighted spectral contribution to an individual principle component. For example, the spectral line 393.36 nm has a high loading value for PC 1 and calcium (393.36 nm) is likely to be an important element that contributes significantly to the discrimination among different kidney stone samples. The loading plot from this analysis is shown in Fig. 4b. It is usually desirable to have data points clustered tightly and clearly separated on the PCA plot for effective sample classification (i.e., sample 4). However, PCA plots can also reveal the elemental heterogeneity within a sample class. If PCA data points are not tightly clustered and spread far apart, (i.e., samples 1, 2, and 3), it is possible to infer that the samples are of high elemental heterogeneity. Furthermore, it may be possible to detect outliers from the data set by observing the extent of deviation from the clustered group; for example, the isolated point in Fig. 4c for sample 4 can be considered as an outlier.

The three-dimensional (3D) PCA chart for the kidney stone samples shows the clustering due to sample similarity. The results for sample 4 (in Fig. 4a) vary greatly from the other samples according to this chart because of its organic matrix structure. PLS-DA data correlate with PCA charts.

In the PLS-DA analysis, sample types 1 through 5 were designated as an individual sample class in the model. The model is then trained to recognize the different sample classes and validated by testing that spectral data associated with a particular sample class match back to their correct class.





c)				Confusion Matrix PLS-DA % 98.41			
	H ₀ -Sample 1	97.5	0	2.5	0	0	[200]
	H ₁ -Sample 2	0	100	0	0	0	[200]
Truth	H ₂ -Sample 3	0	0	98.5	0	0	[200]
	H ₃ -Sample 4	0	0.67	0	99.33	0	[150]
	H ₄ -Sample 5	0	0	28.57	14.29	57.14	[7]
		H ₀	H ₁	H ₂ Response	H ₃	H ₄	

Fig. 4. (a) PCA, (b) loading plot from PC1, 2, and 3, and (c) PLS-DA result for kidney stones using RT100-EC.

Several types of cross-validation methods are available to test and validate PLS-DA models, including full cross-validation, random folds cross-validation, venetian blinds cross-validation, and leave one sample out cross-validation. Each of these methods strategically removes data points from the model, retrains the model, and then tests the removed data back against the re-trained model. In the current study, due to a small number of samples for building the test model, the full cross-validation method in which all kidney stone LIBS data is used to train and evaluate the model was applied.

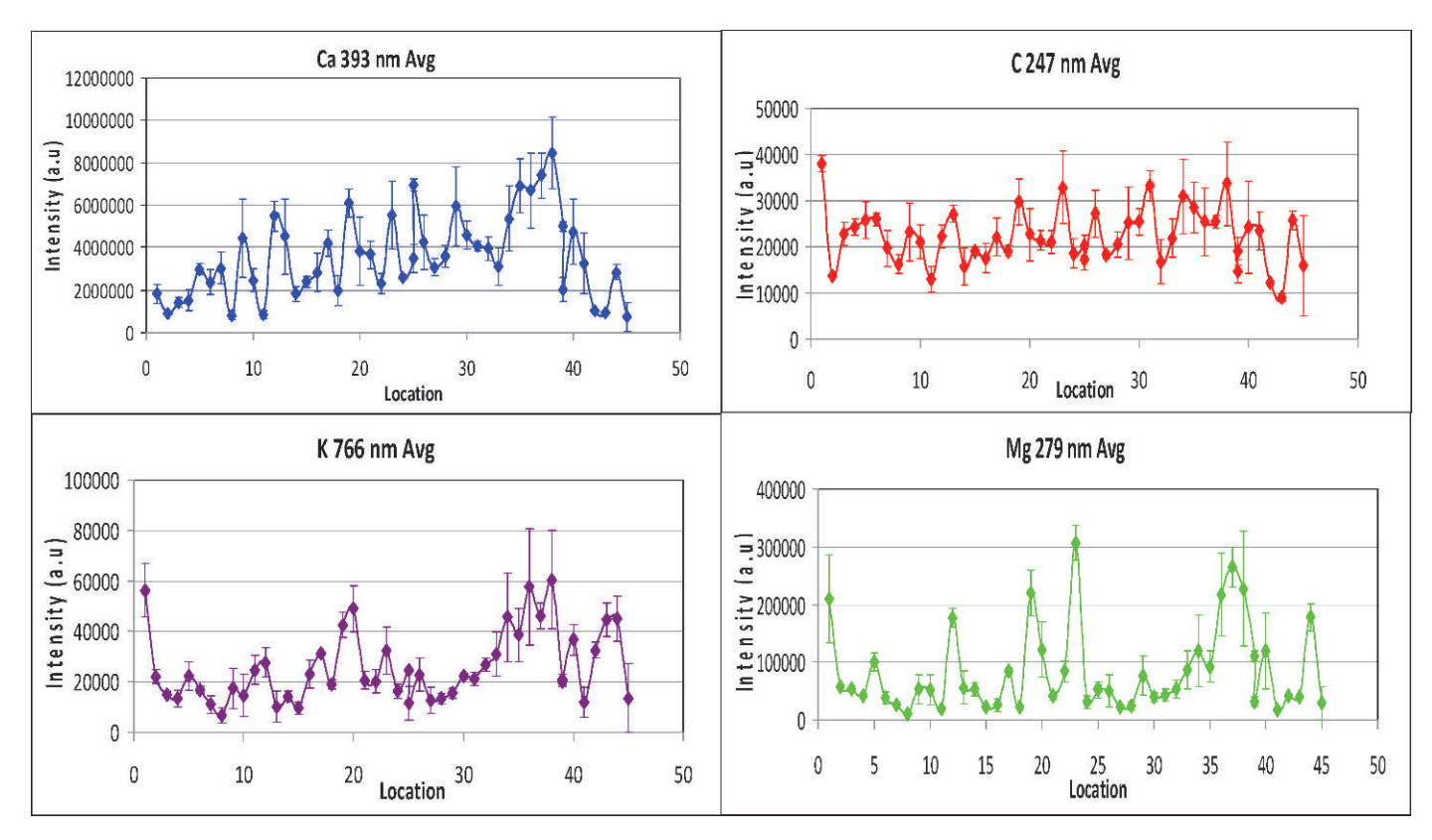


Fig. 5. Line intensities of Ca at 393.4 nm, C at 247.86 nm, K at 766.46 nm, and Mg at 279.80 nm measured at forty-five different locations on the surface of sample 1.

The results from PLS-DA calculations are presented as a confusion matrix in Fig. 4b. This matrix summarizes the percentage of tested samples in a particular sample class that are correctly matched back to their class. From the figure, it can be seen which sample classes are being confused with one another. Overall discrimination efficiency of 98.42% was achieved. However, 1.5% of sample 1 was confused with sample 3, 0.67% of sample 4 was confused with sample 2, 28.57% of sample 5 was confused with sample 3, and 14.29% of sample 5 was confused with sample 4.

The variable importance in projection (VIP) scores are used to estimate the importance of each spectral wavelength in the PLS calculation. Table II shows the ten highest scores and the associated wavelengths. The spectral wavelengths with the highest VIP values are strongly correlated to the PLS-DA results. Items with VIP value between 0 and 1 are not responsible for the correct identification results. Table II shows that the top ten VIP scores are mostly related to Ca and K emission lines and these elements should play a significant role in discriminating different classes of kidney stones.

All samples correlate back to the correct hypothesis with high percentages, with the exception of sample 5. Spectral line intensity ratios of sample 4 are different (see Table III) and are separated easily from organic compounds for sample 4 according to the PCA and PLS-DA results (see Fig. 4).

Elemental profiles were measured using LIBS across two kidney stone samples embedded in resin (sample 1 and 2) as shown in Figs. 5 and 6, respectively. In both samples Ca and C follow the same trend, different from that measured for K and Mg. The two samples are visually different; particularly, sample 2 was more striated (see Fig. 1).

The most widely accepted stone formation mechanism depends on multiple factors such as excessive sun exposure, nutrition, and inadequate fluid intake as well as pH changes in the urine.³⁶ Urinary tract stones (kidney, bladder, and urinary tract) are formed in various organic, inorganic, and semiorganic compounds. The most common kidney stones are urinary tract stones and they are commonly categorized into either organic or inorganic type. Calcium oxalate (whewellitewheddelite), calcium phosphate (hydroxyapatite-brushite) and calcium oxalate-calcium phosphate stones have a mixture of inorganic chemical composition, while the sulfonamide, uric acid, magnesium ammonium phosphate (struvite), cysteine, and xanthine stones have organic chemical composition. In addition, calcium oxalate-uric acid can have both organic and inorganic chemical composition. Dietary habits, genetic factors, metabolic disturbances, climatic conditions, medications, and lifestyle play an important role in the formation of kidney stones. Types of prevalent kidney stones change from country to country or even within the same country due to climate condition variations in different regions. Knowing the type of patients' stones is important in determining suitable treatment methods (ESWL, laser breaking, or percutaneous nephrolithotomy [PNL]), as well as preventing reformation of kidney stones, administrating treatment, disposal methods, and recommending the right diet to patients.

X-ray diffraction analysis to determine the crystal structure and FT-IR for molecular bonds are increasingly being used for kidney stone analysis. XRF, ICP-MS or atomic emission spectroscopy, and SEM-EDX also are commonly used to determine elemental composition. However, the ability of LIBS to classify kidney stones demonstrates a clear advantage with the

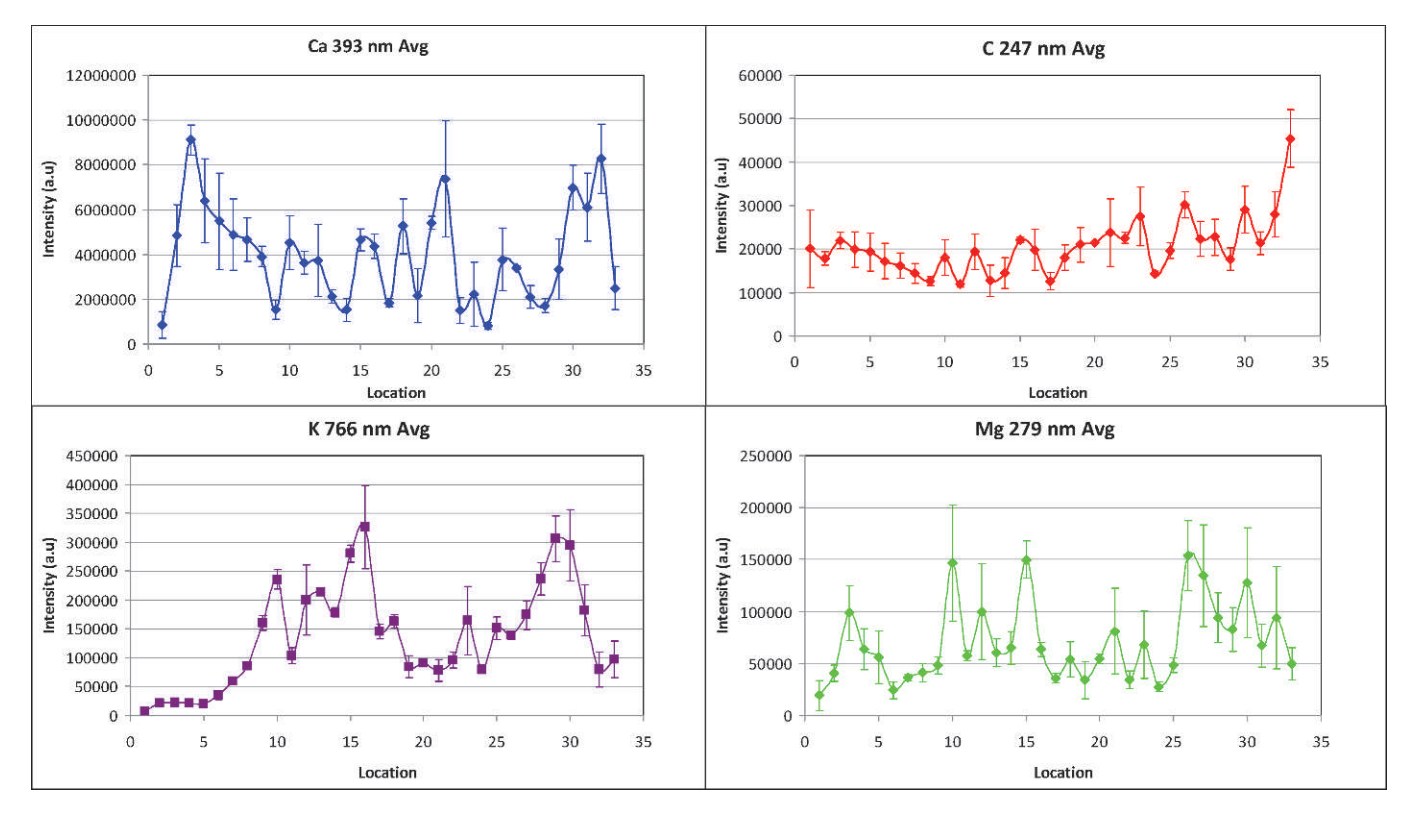


Fig. 6. Line intensities of Ca at 393.4 nm, C at 247.86 nm, K at 766.46 nm, and Mg at 279.80 nm measured at thirty-three different locations on the surface of sample 2.

added simplicity of sample preparation and measurement speed. In this study, samples were first classified with respect to their crystal structure through XRD. XRF was preferred to determine the elemental composition for low concentrations at a level of parts per billion (ppb) but elements such as C, H, and N usually present in organic-type stones could not be observed; hence, no accurate quantitative analysis was possible, especially with organic samples. Elemental composition measured with XRF does not contribute to the classification of kidney stones.

The ability of LIBS to determine the type of kidney stone without any sample preparation, with high speed, and in situ under a clinical setting is expected to significantly aid the medical community in selecting proper treatment and prevention methods for patients. LIBS gives an advantage of carrying out simultaneous elemental analysis and classification of kidney stones using a single instrument, whereas this range of information would only be possible by carrying out separate measurements of XRF and XRD.

CONCLUSIONS

Heterogeneous kidney stones were analyzed by LIBS using a short-pulsed high power laser and high resolution multi-channel CCD spectrometers. Both XRF and XRD techniques require a larger size kidney stone for effective analysis. Furthermore, because the samples have to be ground and prepared in a pellet form, local compositional information of the samples is lost with XRD and XRF techniques. On the other hand, with LIBS, a laser beam can be focused on a sample surface with a spot size less than a few tens of micrometers to achieve high spatial resolution. Formation of kidney stones takes place over a long period of

time causing heterogeneous distribution of various elements within the same stone.

This paper demonstrates LIBS as a promising, simple, and accurate analytical method for the characterization of kidney stones. LIBS emission lines characteristic of elements present in five different types of kidney stones were detected at different locations of the stones, producing elemental mapping. The lighter elements critical to kidney stone classification such as C, H, and N were also detected with ease by LIBS and not by XRF. The classification of the stones was conducted using the spectral line intensity ratios of C, H, Ca, Mg, and P elements. The 3D view of the PCA chart showed clustering characteristics with respect to whether a stone was of organic/ inorganic nature or mixed. Whewellite (CaC₂O₄·H₂O), wheddelite (CaC₂O₄·2H₂O), hydroxyapatite Ca₁₀(PO4)₆(OH)₂, and uric acid (C₅H₄N₄O₃) compounds were present at different compositions in the stones with crystalline structure composed of Ca, C, O, H, and P elements. A LIBS system has advantages for rapid analysis of kidney stones compared to XRD and XRF. LIBS also provides a measure of spatial distribution of elements in the samples.

ACKNOWLEDGMENTS

This work is supported by the State Planning Organization of Turkey, Kocaeli University Research Fund, and the Ministry of Science, Industry and Technology of Turkey under contracts 2011K120330, 2010/96 and 404.TGSD.2010 projects, respectively.

V. Uvarov, I. Popov, N. Shapur, T. Abdin, O.N. Gofrit, D. Pode, M. Duvdevani. "X-Ray Diffraction and SEM Study ff Kidney Stones in Israel: Quantitative Analysis, Crystallite Size Determination, and Statistical Characterization". Environ. Geochem. Health. 2011. 33: 613-622.

^{2.} I. Oswald, S. Cavalu, T.T. Maghiar, D. Osvat. "Identification of the

- Urinary Stone Composition upon Extracorporeal Shock Wave Lithotripsy". Romanian J. Biophys. 2011. 21(2): 107-112.
- D.A. Cremers, L.J. Radziemski. "Handbook of Laser-Induced Breakdown Spectroscopy". New York: Wiley, 2006.
- A.W. Miziolek, V. Palleschi, I. Schchter. "Laser-Induced Breakdown Spectroscopy (LIBS): Fundamentals and Applications". Cambridge. 2006.
- M. Baudelet, M. Boueri, J. Yu, S.S. Mao, V. Piseltelli, X.L. Mao, R.E. Russo. "Time-Resolved Ultraviolet Laser-Induced Breakdown Spectroscopy for Organic Material Analysis". Spectrochim. Acta, Part B. 2007. 62: 1329-1334.
- J. Li, J. Lu, Z. Lin, S. Gong, C. Xie, L. Chang, L. Yang, P. Li. "Effects of Experimental Parameters on Elemental Analysis of Coal by Laser-Induced Breakdown Spectroscopy". Opt. Laser Technol. 2009. 41(8): 907-913.
- J.P. Singh, S.N. Thakur. "Laser-Induced Breakdown Spectroscopy". Netherlands: Elsevier, 2007.
- V.K. Singh, V. Singh, A.K. Rai, S.N. Thakur, P.K. Rai, J.P. Singh. "Quantitative Analysis of Gallstones Using Laser-Induced Breakdown Spectroscopy". Appl. Opt. 2008. 47(31): G38-G47.
- M. Baudelet, M. Boueri, J. Yu, X. Mao, S.S. Mao, R. Russo. "Laser Ablation of Organic Materials for Discrimination of Bacteria in an Inorganic Background". Proc. SPIE. 2009. 7214: 72140J1-9.
- M.A. Kasem, R.E. Russo, M.A. Harith. "Influence of Biological Degradation and Environmental Effects on the Interpretation of Archeological Bone Samples with Laser-Induced Breakdown Spectroscopy". J. Anal. At. Spectrom. 2011. 26: 1733-1739.
- X. Fang, S.R. Ahmad, M. Mayo, S. Iqbal. "Elemental analysis of urinary calculi by laser induced plasma spectroscopy". Lasers Med. Sci. 2005. 20: 132-137.
- V.K. Singh, A.K. Rai, P.K. Rai, P.K. Jindal. "Cross-sectional study of kidney stones by laser-induced breakdown spectroscopy". Lasers Med. Sci. 2009. 24: 749-759.
- J. Anzano, R.J. Lasheras. "Strategies for the identification of urinary calculus by laser induced breakdown spectroscopy". Talanta. 2009. 79: 352-360.
- NIST Atomic Spectra Database Lines Form. http://physics.nist.gov/ PhysRefData/ASD/lines_form.html. [accessed Feb 15 2012].
- J.D. Hybl, G.A. Lithgow, S.G. Buckley. "Laser-Induced Breakdown Spectroscopy Detection and Classification of Biological Aerosols". Appl. Spectrosc. 2003. 57(10): 1207-1215.
- A.C. Samuels, F.C. Delucia, K.L. Mcnesby, A.W. Miziolek. "Laser-Induced Breakdown Spectroscopy of Bacterial Spores, Molds, Pollens, and Protein: Initial Studies of Discrimination Potential". Appl. Opt. 2003. 42: 6205-6209.
- J.B. Sirven, B. Salle, P. Mauchien, J.L. Lacour, S. Maurice, G. Manhes. "Feasibility Study of Rock Identification at the Surface of Mars by Remote Laser-Induced Breakdown Spectroscopy and Three Chemometric Methods. J. Anal. Atom". Spectrom. 2007. 22: 1471-1480.
- A.A. Bol'shakov, J.H. Yoo, C. Liu, R.E. Russo. "LIBS Security Applications at the United States Army Research Laboratory". Spectroscopy. 2009. 24: 32-38.
- A.K. Myakalwar, S. Sreedhar, I. Barman, N.C. Dingari, S.V. Rao, P.P. Kiran, S.P. Tewari, G.M. Kumar. "Laser-Induced Breakdown Spectroscopy-Based Investigation and Classification of Pharmaceutical Tablets Using Multivariate Chemometric Analysis". Talanta. 2011. 87: 53-59.
- 20. M.R. Martelli, F. Brygo, A. Sadoudi, P. Delaporte, C. Barron, J. Agric.

- "Laser-Induced Breakdown Spectroscopy and Chemometrics: A Novel Potential Method to Analyze Wheat Grains". Food Chem. 2010. 58(12): 7126-7134.
- A. Koujelev, M. Sabsabi, V. Motto-Ros, S. Laville, S.L. Lui. "Laser-Induced Breakdown Spectroscopy with Artificial Neural Network Processing for Material Identification. Planet". Space Sci. 2010. 58: 682-690.
- V.B. Nalbandyan. "X-Ray Diffraction Analysis of Urinary Calculi: Need for Heat Treatment". Urol. Res. 2008. 36: 247-249.
- G. Kanchana, P. Sundaramoorthi, G.P. Jeyanthi. "Bio-Chemical Analysis and FTIR-Spectral Studies of Artificially Removed Renal Stone Mineral Constituents". J. Miner. Mater. Character. Eng. 2009. 8: 161-170.
- 24. S.H. Lee, H.S. Shim, J.H. Yoo, R.E. Russo, S.H. Jeong. "Analysis of the Absorption Layer of CIGS Solar Cell by Laser-Induced Breakdown Spectroscopy". The 3rd North American Symposium on Laser-Induced Breakdown Spectroscopy. Florida, USA: NASLIBS, 2011. July 18-20, 2011.
- B. Genc Oztoprak, E. Akman, M.M. Hanon, M. Gunes, S. Gumus, E. Kacar, O. Gundogdu, M. Zeren, A. Demir. J. Opt. Laser Technol. 2012. http://dx.doi.org/10.1016/j.optlastec.2012.05.001.
- J.L. Meyer, E.E. Angino. "The Role of Trace Metals in Calcium Urolithiasis". Invest. Urol. 1977. 14: 347-350.
- T. Ozgurtas, G. Yakut, M. Gulec, M. Serdar, T. Kutluay. "Role of Urinary Zinc and Copper on Calcium Oxalate Stone Formation". Urol. Int. 2004. 72(3): 233-236.
- A. Trinchieri, A. Mandressi, P. Luongo, G. Longo, E. Pisani. "The influence of diet on urinary risk factors for stones in healthy subjects and idiopathic renal calcium stone formers". Br. J. Urol. 1991. 67: 230-236.
- I.H. Atakan, M. Kaplan, G. Seren, T. Aktoz, H. Gul, O. Inci. "Serum, Urinary and Stone Zinc, Iron, Magnesium And Copper Levels in Idiopathic Calcium Oxalate Stone Patients". Int. Urol. Nephrol. 2007. 39(2): 351-356.
- J.C. Anderson. Quantitative and Qualitative Investigations Into Urinary Calculi Using Infrared Microspectroscopy, [Doctor of Science in Technology Dissertation]. Oxford, OH: Miami University, 2007.
- T. Kakhia. Health effects of copper, tarek.kakhia.org/periodic_table/ english/Copper. [accessed Feb 15 2012].
- Agency for Toxic Substances and Disease Registry, Toxicological Profile for Copper, U.S. Department Of Health And Human Services. 1990. http:// www.seagrant.umn.edu/water/report/chemicalsofconcern/copper/copper. pdf. [accessed Feb 15 2012].
- M. Tran, Q. Sun, B.W. Smith, J.D. Winefordner. "Direct Determination of Trace Elements in Terephthalic Acid by Laser Induced Breakdown Spectroscopy". J. Anal. Atom". Spectrom. 2001. 16: 628-632.
- C. López-Moreno, S. Palanco, J.J. Laserna, F. DeLucia, A.W. Miziolek, J. Rose, R.A. Walters, A.I. Whitehouse. "Test of a Stand-Off Laser-Induced Breakdown Spectroscopy Sensor for the Detection of Explosive Residues on Solid Surfaces". J. Anal. Atom. Spectrom. 2006. 21: 55-60.
- 35. R.S. Harmon, K.M. Shughrue, J.J. Remus, M.A. Wise, L.J. East, R.R. Hark. "Can The Provenance of the Conflict Minerals Columbite and Tantalite be Ascertained by Laser-Induced Breakdown Spectroscopy?". Anal. Bioanal. Chem. 2011. 400: 3377-3382.
- F. Grases, A. Costa-Bauzá, L. García-Ferragut. "Biopathological Crystallization: A General View About The Mechanisms of Renal Stone Formation". Adv. Colloid Interface Sci. 1998. 74: 169-194.